Available online at www.sciencedirect.com

ScienceDirect

Catalysis Today 118 (2006) 144–150

CATALYSIS TODAY

www.elsevier.com/locate/cattod

Initiation of oxygen permeation and POM reaction in different mixed conducting ceramic membrane reactors

Jianhua Tong [a,b,*], Weishen Yang [a], Hiroyuki Suda [b], Kenji Haraya [b]

[a] State Key Laboratory of Catalysis, Dalian Institute of Chemical Physics, Chinese Academy of Sciences,
P.O. Box 110, 457 Zhongshan Road, 116023 Dalian, China
[b] Research Institute for Innovation in Sustainable Chemistry, National Institute of Advanced Industrial Science and Technology (AIST),
Central 5, 1-1-1 Higashi, 305-8565 Tsukuba, Japan

Available online 13 July 2006

Abstract

The initiation of oxygen permeation and POM were studied in mixed conducting ceramic membrane reactors. Membrane material composition, and catalyst-loading mode were proven to have an important effect on the initiation of oxygen permeation and POM reaction. The initiation time for compositions of $Ba_{0.5}Sr_{0.5}Co_{0.8}Fe_{0.2}O_{3-\delta}$ (BSCFO) and $BaCo_{0.4}Fe_{0.4}Zr_{0.2}O_{3-\delta}$ (BCFZO) are 20 and 2 h, respectively. When the catalyst was loaded directly on the membrane surface the oxygen permeation flux increased 8–10-fold of that under air/He gradient. The good POM performance of the methane conversion, higher than 96% and the CO selectivity, higher than 95%, was achieved successfully. However, when the catalyst was loaded on a place away from the membrane surface or the catalyst was not loaded, the lower oxygen permeation flux (1–2-fold) and the poor POM performance (the methane conversion is lower than 30% and the CO selectivity is lower than 20%) were obtained. The characterization of XRD and SEM-EDS indicated that the initial process might be finished through initiating the catalyst and adjusting the membrane structure (the formation of a thin CoO containing porous layer with a thickness of about 10 μm). The great increase of oxygen permeation flux can be ascribed to the great decrease of the oxygen partial pressure and the adjustment of the surface structure.

Keywords: Oxygen permeation; POM reaction; Ceramic membrane reactor

1. Introduction

In recent years, mixed conducting ceramic membrane reactors have attracted rapidly increased attention owing to their application to separate pure oxygen from an oxygen mixture, to produce synthesis gas from the catalytic membrane reaction (partial oxidation of methane, POM), and to supply special oxygen species for some selective oxidation reactions [1–10]. Besides the extensive study of the mixed conducting materials [11–18], the POM in membrane reactor is the most prevalent research, owing to the great industrial motivation of GTL (gas to liquid) [5–8,19–23]. Balachandran et al. investigated the membrane reactors constructed from $La_{0.2}Sr_{0.8}Co_{0.8}Fe_{0.2}O_{3-\delta}$, $SrCo_{0.8}Fe_{0.2}O_{3-\delta}$, or $SrCo_{0.5}FeO_x$ [5,19]. Tsai et al. made a disk-shape membrane reactor from $La_{0.2}Ba_{0.8}Fe_{0.8}Co_{0.2}O_{3-\delta}$, in which the long-term stable operation of 850 h was obtained [6]. In our previous work, the disk-shape and tube-shape membrane reactors were constructed from $Ba_{0.5}Sr_{0.5}Co_{0.8}Fe_{0.2}O_{3-\delta}$ (BSCFO) and $BaCo_{0.4}Fe_{0.4}Zr_{0.2}O_{3-\delta}$ (BCFZO) and POM was carried out. In both membrane reactors, the methane conversion of 98% and the CO selectivity of 99% were obtained successfully (Fig. 1). An oxygen permeation flux as high as 10.45 ml/cm^2 min was achieved in a BSCFO membrane reactor, which is 8–10-fold of that under air/He gradient. The operating time as long as 2200 h was obtained in a BCFZO membrane reactor [8,20–22]. In the present study, we found that it took different times to initialize the oxygen permeation and the POM in different membrane reactors. From an industrial point of view, this initiation is a vital prerequisite to the operation of catalytic membrane reactors. Therefore, the initiation of the oxygen permeation and the POM in membrane reactors constructed from BSCFO and BCFZO were investigated in detail. The initial mechanism was characterized, proposed, and interpreted.

---

* Corresponding author at: Membrane Separation Processes Group, Research Institute for Innovation in Sustainable Chemistry, National Institute of Advanced Industrial Science and Technology (AIST), Central 5, 1-1-1 Higashi, 305-8565 Tsukuba, Japan. Tel.: +81 29 861 4675; fax: +81 29 861 4675.
E-mail address: jhtong2002@hotmail.com (J. Tong).

0920-5861/$ – see front matter © 2006 Elsevier B.V. All rights reserved.
doi:10.1016/j.cattod.2006.02.089

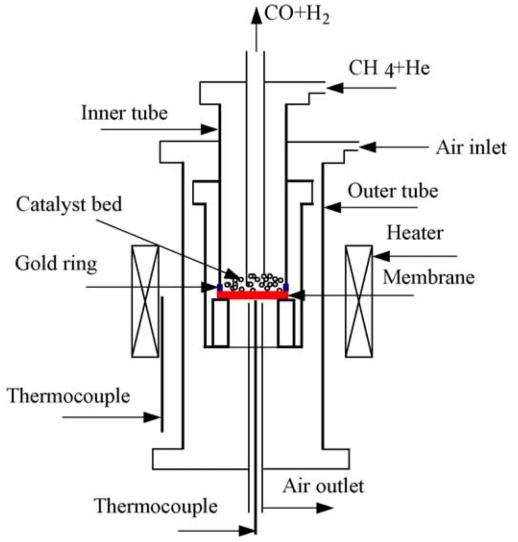

Fig. 1. The schematic of MIECM reactor for POM.

2. Experimental

2.1. Membrane powder

BSCFO and BCFZO powders were synthesized from nitrates of component metals through a method of combining EDTA and citric acid complexes. In brief, the calculated amounts of nitrates were dissolved in EDTA-$NH_3 \cdot H_2O$ solution under heating and stirring. Then, the proper amount of citric acid was introduced, the mole ratio of EDTA acid:citric acid:total metal ions was controlled to be around 1:1.5:1. Precipitation might occur after citric acid addition, $NH_3 \cdot H_2O$ or HNO_3 was added to adjust the pH value to around 6, and the solution became transparent immediately. With the evaporation of water, a dark purple gel was achieved. The gel was then treated at 120 °C for 10 h to get primary powders, which were calcined at 950 °C for 5 h to obtain powders with final composition [4,16].

2.2. Membrane disk

The as-synthesized powders were compressed into disks in a stainless steel mold (17 mm in diameter) under a hydraulic pressures of 15–25 MPa based on an area of 2.27 cm^2. Green disk compacts were then sintered in air at 1100–1200 °C for 10 h, with heating and cooling rates of 1 and 2 °C min^{-1}, respectively. The densities of the sintered membrane disks were determined by the Archimedes method using ethanol. Only those membrane disks that had relative densities higher than 95% were used for permeation study and constructing the membrane reactor.

2.3. Membrane reactor

After polishing on both surfaces, the membrane disk was mounted on a quartz tube using a gold ring seal. Then, the temperature was increased to 1070 °C and maintained at this temperature for several minutes. After sealing the membrane disk well, the temperature was cooled down to 850 °C at a rate of 1 °C min^{-1}. The membrane reaction was carried out in the modes of A–C shown in Fig. 2. The diluted methane (50% He and 50% CH_4) was used as feed. A HP6890A gas chromatograph was used for analyzing the composition of the product. A 5A molecular sieve column was used for the separation of H_2, O_2, N_2, CH_4 and CO. A TDX-01 column was used for the separation of CO, CO_2 and hydrocarbons.

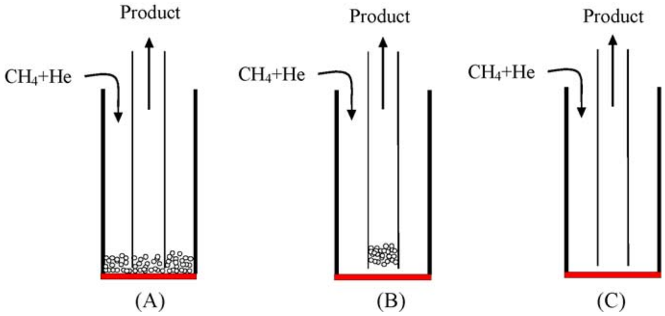

Fig. 2. The operating modes of membrane reactors for POM.

2.4. Designated membrane reaction

The initiation of BSCFO membrane reactor in operating mode A was carried out as follows: after sealing the membrane reactor well, the operating temperature was kept at 850 °C; 300 mg catalyst was loaded on the membrane disk surface; CH_4 feed (diluted by 50% He) with a rate of 35 ml/min and air with a rate of 300 ml/min were introduced into this membrane reactor. The initiation of the BCFZO membrane reactor in operating mode A was carried out under similar conditions with those for the BSCFO membrane reactor except that the CH_4 feed rate was 24 ml/min rather than 35 ml/min. The different CH_4 feed rates are chosen according to the different oxygen permeation flux under the air/He gradient.

In comparison, the POM was also carried out in the BSCFO membrane reactor in the operating modes B and C. The temperature was kept at 850 °C. The CH_4 feed with a rate of 30 ml/min and the air feed with a rate of 300 ml/min were introduced into the membrane reactors. The experiments were carried out for 50 h.

2.5. Characterization

XRD (Rigaku D/MAX-RB, Cu Kα) was used to characterize the BSCFO membrane disks after reaction for 50 h in membrane reaction with operating modes A and C. SEM-EDS (JEM-5600LV, Oxford ISIS-300) was also used to characterize the morphology and the composition of these membrane disks.

3. Results and discussion

3.1. Initiation of oxygen permeation and POM reaction in membrane reactors

3.1.1. Effect of membrane composition on initiation in operating mode A

The initiation results of oxygen permeation and POM reaction in BCFZO membrane reactor are shown in Fig. 3. At

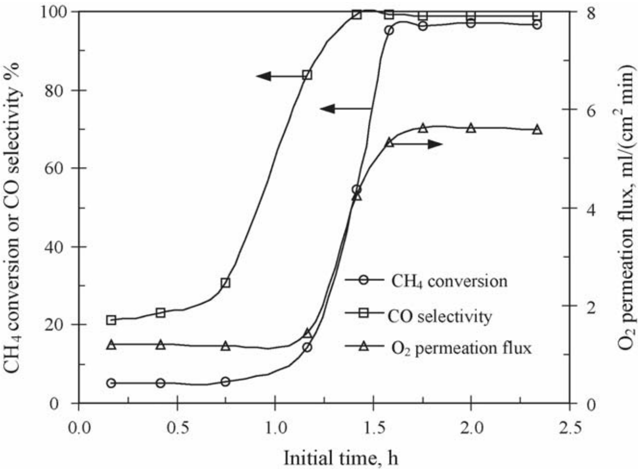

Fig. 3. Initial process of BCFZO MIECM reactor for POM.

the beginning stage ($t = 0.2$ h), the oxygen flux ($J_{O_2} = 1.19\,\mathrm{ml/cm^2\,min}$) is two times as that under air/He gradient ($J_{O_2} = 0.60\,\mathrm{ml/cm^2\,min}$). The CH_4 conversion and the CO selectivity are lower than 5% and 20%, respectively. With increasing initial time, the CO selectivity increases rapidly, almost 100% CO selectivity has been achieved at $t = 1.3$ h. The rocket increase of the oxygen flux and the CH_4 conversion is a little delayed, which begins at $t = 1.2$ h and finishes at $t = 1.7$ h. Within 2.0 h, CH_4 conversion of 98%, CO selectivity of 99%, and oxygen flux of 5.6 ml/cm^2 min (9.3 times as the value under air/He gradient) are achieved for the BCFZO membrane reactor.

The initiation results of oxygen permeation and POM reaction in the BSCFO membrane reactor are shown in Fig. 4. At the beginning stage ($t = 1.1$ h), the oxygen flux ($J_{O_2} = 1.68\,\mathrm{ml/cm^2\,min}$) is just a little higher than that under air/He gradient ($J_{O_2} = 1.20\,\mathrm{ml/cm^2\,min}$). The CH_4 conversion is lower than 10%, and the CO selectivity is lower than 22%. With the increase in initial time, the oxygen flux slowly increases to 2.1 ml/cm^2 min ($t = 7.5$ h), 25% higher than the start value. The increasing rate of the CH_4 conversion is a little quicker than that of the oxygen flux, about 40% CH_4 has been converted at $t = 7.5$ h. The CO selectivity increases rapidly, almost 100% at $t = 7.5$ h. At the stage of 7.5–12.5 h, the CH_4 conversion rockets to 97% from 40% accompanied with a sharp increase in the oxygen flux ($J_{O_2} = 9.52\,\mathrm{ml/cm^2\,min}$). But the CO selectivity decreases a little (95%). The increasing rate of the oxygen flux decelerates after $t = 12.5$ h and levels off after 20 h. At last, the CH_4 conversion of 98%, the CO selectivity of 93%, and the oxygen flux of 10.5 ml/cm^2 min (8.8 times as the value under air/He gradient) are achieved for BSCFO membrane reactor. In comparing the initiation in two membrane reactors, it can be easily found that the initial time of 2 h in BCFZO membrane reactor is much faster than that of 20 h in BSCFO membrane reactor.

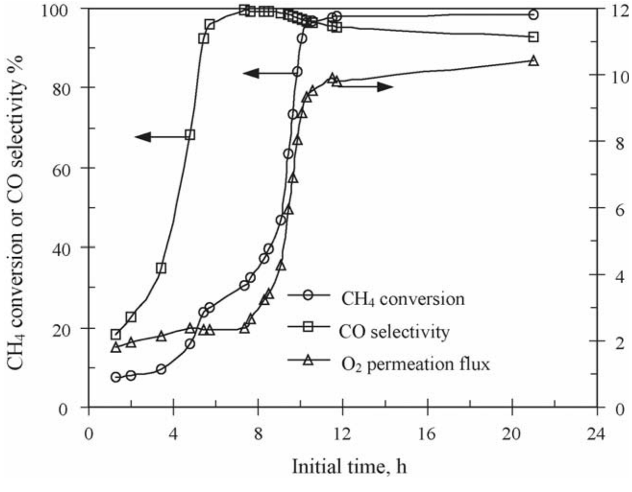

Fig. 4. Initial process of BSCFO MIECM reactor for POM.

3.1.2. Effect of operating modes on the initiation

In order know the initiation mechanism, the initiation in operating mode B and operating mode C were also measured. In operating modes B and C, after having introduced methane for 50 h the oxygen permeation flux is just a little higher than that under the air/He gradient. The CH_4 conversion is lower than 20%, the main carbon-containing products are CO_2 and C_2 rather than CO. Moreover, the H_2 concentration in the product is very small. The main reaction is the complete oxidation and coupling oxidation rather than POM. It is obvious that the oxygen flux has not been greatly increased.

3.2. Characterization

The SEM images of the surface and the cross-section of both sides of the BSCFO membrane after initiation in operating mode A for 50 h are shown Fig. 5. The reaction side surface was destroyed greatly and a porous layer was formed. There are some large bulges on the membrane surface, which were proven to be carbonate by EDS. Many small particles are also found on the membrane surface, which were proven CoO by EDS. The XRD patterns (Fig. 6) also gave evidence that the carbonates and the CoO were formed after initiation in the B mode membrane reactor. The cross-section image of the membrane near reaction side shows that the porous layer is about 10 μm. Away from the reaction side the membrane is kept at the same morphology and structure as the fresh membrane. On the other hand, the airside SEM images show that the morphology and structure of the surface and the cross-section are same as the fresh membrane, evidenced by XRD patterns. The SEM images of the surface and the cross-section of both sides of the BSCFO membrane after initiation in operating mode B for 50 h are shown in Fig. 7. The surface morphology of both sides of the initiated membrane is almost the same as the fresh membrane except for a few needle-shape particles. The XRD patterns (Fig. 8) indicate that the perovskite structure is still kept for the initiated membrane. Therefore, it can be concluded that hardly any change took place in the membrane after reacting for 50 h in the BSCFO membrane reactor of operating mode B. This can be used to explain the smaller oxygen permeation flux and the lower CH_4 conversion. Overall, it can be

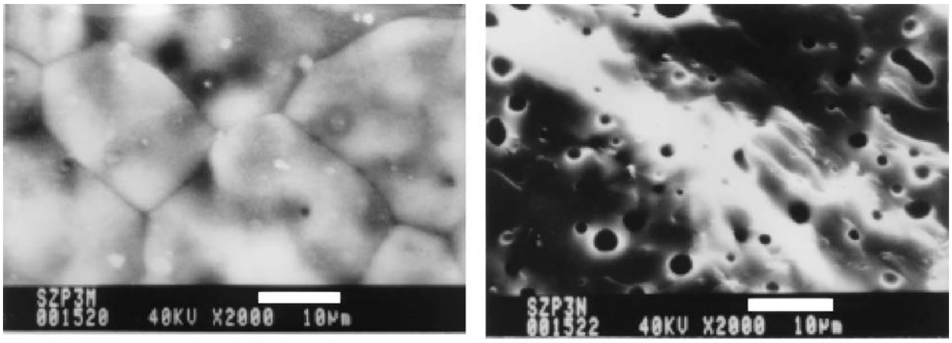

(a) Top view of fresh disk

(b) Cross section of fresh disk

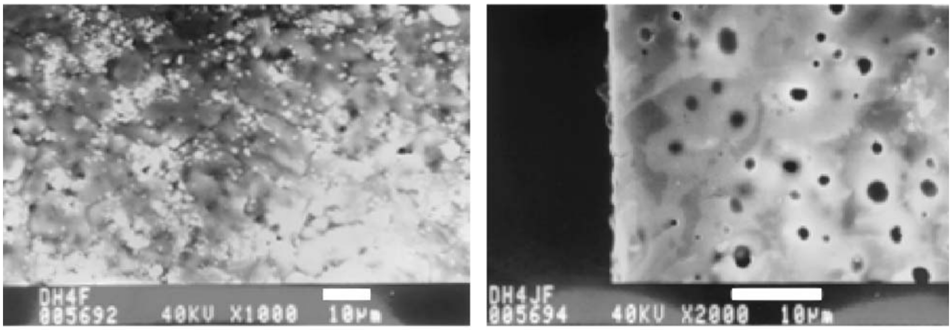

(c) Top view of air side disk

(d) Cross section of air side disk

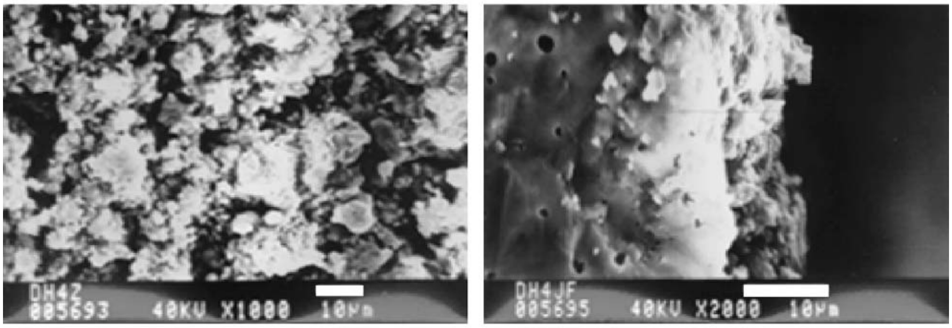

(e) Top view of reaction side disk

(f) Cross section of reaction side disk

Fig. 5. Morphology of surface and cross-section of BSCFO membrane disk before initiation and after initiation in operating mode A for 50 h. (a) Top view of airside disk; (b) cross-section of airside disk; (c) top view of reaction side disk; (d) cross-section of reaction side disk; (e) top view of reaction side disk; (f) cross-section of reaction side disk.

concluded that the BSCFO membrane reactor can be initiated successfully in operating mode A rather than in operating mode B accompanied by the surface the adjustment of the surface structure and morphology.

3.3. Initiation mechanism

3.3.1. Two-stage initiation mechanism

The LiLaNiO/γ-Al_2O_3 catalyst was used in our MIECM reactors for POM. The supported nickel on this catalyst is in the oxidized state, $NiAlO_4$, which is active for methane combustion. This may give a good reason why CO_2 selectivity is high at the beginning. The initial reduction of $NiAlO_4$ to Ni_0 starts slowly, but once some Ni_0 appears, the reduction process is accelerated by the produced H_2 and CO. The reduction of $NiAlO_4$ to Ni_0 and the production of H_2 and CO accelerate each other, which results in the rapid increase of the CO selectivity and H_2 production. The initiation process of the LiLaNiO/γ-Al_2O_3 catalyst can be finished within 1 h in the traditional reactor. Considering the gradual supply of oxygen through the oxygen permeation membrane, this catalyst initial process in MIECM reactors may be delayed a little.

With the increase of H_2 and CO amount in the reaction mixture, the membrane surface was reduced and a porous CoO containing layer was gradually formed, resulting in a great increase in the membrane surface area. The as-resulted CoO small particles not only can greatly increase the oxygen surface exchange rate, but also can be used as an oxidation catalyst. The rate of the membrane structure adjustment is very different for different membrane materials. As for the BCFZO membrane, the structure adjustment is fast, it just takes 2 h to finish the whole initiation process. As for the BSCFO membrane, the structure adjustment takes 10 times as long as that for the

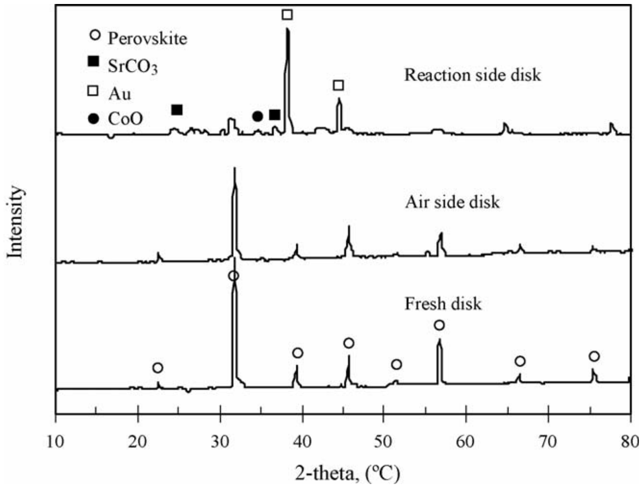

Fig. 6. XRD patterns of BSCFO membrane disk before and after initiation in operating mode A for 50 h.

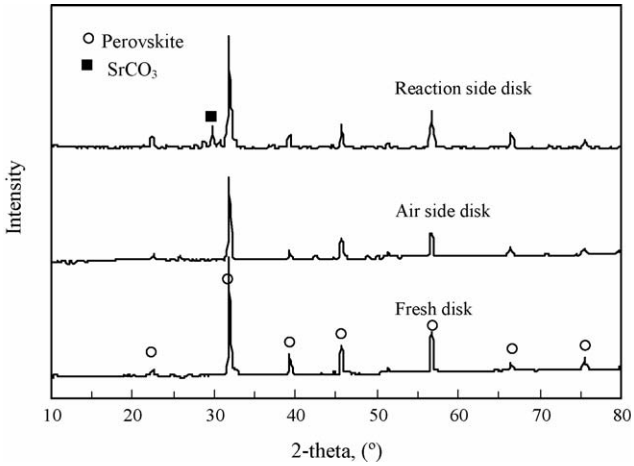

Fig. 8. XRD patterns of BSCFO membrane disks before and after initiation in operating mode B for 50 h.

BCFZO membrane. The large difference of the initial times may result from the different CO_2 resistivity of different membrane materials. In the initial stage (catalyst initiation), the large amount of CO_2 poisoned the membrane surface by forming a dense carbonate layer. The layer has to be removed or made porous in the process of structure adjustment. By introducing 30% CO_2 into the helium sweep gas at 850 °C, the oxygen flux of BSCFO membrane was decreased to 2% of its original value, and it took 3.5 h completely to recover at 1000 °C after changing to pure helium. Under the same CO_2 treatment condition, the oxygen flux of BCFZO membrane was decreased to 13% of its original value, which is several times larger than that for the BSCFO membrane. It can be recovered completely within 0.5 h at a relatively lower temperature of 850 °C after changing to pure helium. It is obvious that BCFZO has a better CO_2 resistivity than BSCFO, making it much easier to adjust the surface structure to increase the oxygen exchange rate:

$$J_{O_2} = \frac{k_r(P''^{-0.5}_{O_2} - P'^{-0.5}_{O_2})}{\frac{2Lk_f}{D_v} + P'^{-0.5}_{O_2} + P''^{-0.5}_{O_2}} \tag{1}$$

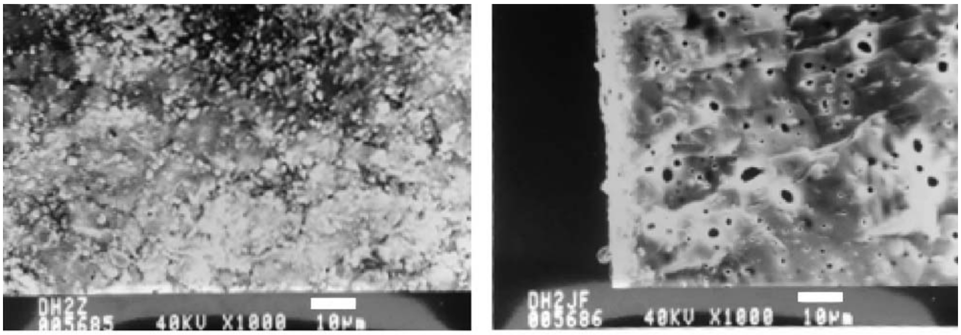

(a) Top view of air side disk (b) Cross section of air side disk

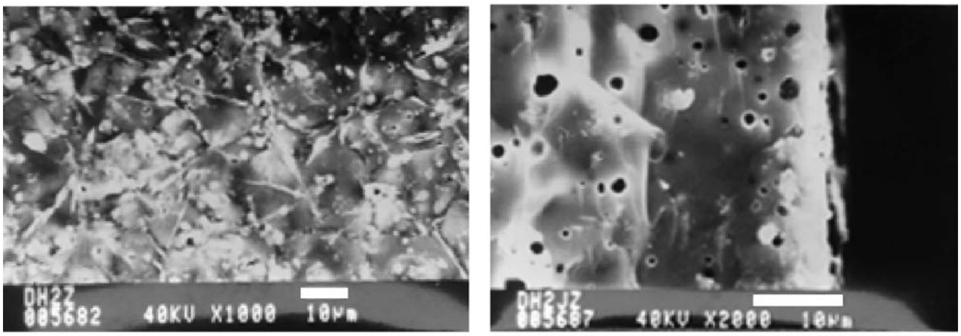

(c) Top view of reaction side disk (d) Cross section of reaction side disk

Fig. 7. Morphology of surface and cross-section of BSCFO membrane disk after initiation in operating mode B for 50 h. (a) Top view of airside disk; (b) cross-section of airside disk; (c) top view of reaction side disk; (d) cross-section of reaction side disk.

3.3.2. Great increase of the oxygen permeation flux

The steady oxygen flux of both BSCFO and BCFZO membrane reactors for POM is 8–10-fold of that under the air/helium gradient. Xu and Thomson [2] developed an explicit oxygen permeation model for mixed conducting membrane reactor (Eq. (1)). Where J_{O_2} is the oxygen permeation flux (mol/m^2 s), k_r reverse surface exchange rate constant (mol/m^2 s), L the membrane thickness (m), k_f forward surface exchange rate constant (m/atm$^{0.5}$ s), P'_O oxygen partial pressure at oxygen-rich side (atm), P''_O the oxygen partial pressure at oxygen-lean side (atm), and D_v is oxygen vacancy bulk diffusion coefficient (m^2/s). The surface exchange kinetics at each side of membrane was studied and the resistance to oxygen permeation was related to the oxygen partial pressure. With the great decrease of the oxygen partial pressure in oxygen-lean side, both the oxygen partial pressure driving force and the oxygen permeation resistance increase greatly, and Eq. (1) can be simplified to $J_{O_2} = k_r$. The oxygen permeation process was mainly controlled by the oxygen exchange rate at oxygen-lean side. k_r is a sensitive function of surface structure. A modification factor of α was introduced to indicate the effect of the surface structure change on the oxygen permeation behavior. For example, α value of 1.67 was used to modify the k_r value resulted from minor surface structure difference by different membrane preparation process. In the case of our membrane reaction for POM, the reaction rate is extremely rapid. The permeated oxygen can be consumed immediately; the oxygen partial pressure is greatly lower than that in airside. Therefore, the oxygen flux is determined by the oxygen exchange rate at the reaction side surface. In the initial process, a porous layer was formed gradually on the membrane surface, which has greatly increased the modification factor of α. The k_r value (oxygen flux) increases greatly under the membrane reaction conditions. The great increase of the oxygen flux resulted from the larger α value due to the formation of thin porous surface layer is reasonable considering the α value of 1.67 for the smaller surface change. In fact, Akin and Lin [24] set up a simple math model for an MIECM reactor for selective oxidation of ethane using a changing oxygen permeation equation, and the effect of reaction conditions on the oxygen flux was simulated in detail. The oxygen flux also increased several-fold compared with that under the air/inert sweep gas gradient.

4. Conclusion

Using membrane reactors constructed from perovskite oxides of BSCFO and BCFZO, the initial process of the catalytic membrane reaction for POM was investigated, characterized, and interpreted. Initial times of 2 and 20 h were needed for the BCFZO and BSCFO membrane reactors, respectively. CH_4 conversion of 98%, CO selectivity of 99%, and oxygen flux of 5.6 ml/cm^2 min (9.3 times of the value under the air/He gradient) are achieved for the BCFZO membrane reactor. CH_4 conversion of 98%, CO selectivity of 93%, and oxygen flux of 10.5 ml/cm^2 min (8.8 times of the value under the air/He gradient) are achieved for the BSCFO membrane reactor. The initial process was finished through initiating the catalyst and adjusting the membrane surface structure by forming a thin porous layer.

References

[1] H.J.H. Bouwmeester, A.J. Burggraaf, Dense ceramic membranes for oxygen separation, in: A.J. Burggraaf, L. Cot (Eds.), Fundamentals of Inorganic Membrane Science and Technology, Elsevier, Amsterdam, 1996, pp. 435–528.

[2] S.J. Xu, W.J. Thomson, Oxygen permeation rates through ion-conducting perovskite membranes, Chem. Eng. Sci. 54 (1999) 3839–3850.

[3] P.V. Hendriksen, P.H. Larsen, M. Mogensen, F.W. Poulsen, K. Wiik, Prospects and problems of dense oxygen permeable membranes, Catal. Today 56 (2000) 283–295.

[4] Z.P. Shao, W.S. Yang, Y. Cong, H. Dong, J.H. Tong, G.X. Xiong, Investigation of the permeation behavior and stability of $Ba_{0.5}Sr_{0.5}Co_{0.8}Fe_{0.2}O_{3-\delta}$ oxygen membrane, J. Membr. Sci. 172 (2000) 177–188.

[5] U. Balachandran, J.T. Dusek, R.L. Mieville, R.B. Poeppel, M.S. Kleefisch, S. Pei, T.P. Kobylinski, C.A. Udovich, A.C. Bose, Dense ceramic membranes for partial oxidation of methane to syngas, Appl. Catal. A 133 (1995) 19–29.

[6] C.Y. Tsai, A.G. Dixon, W.R. Moser, Y.H. Ma, Dense perovskite membrane reactors for partial oxidation of methane to syngas, AIChE J. 43 (1997) 2741–2750.

[7] C.S. Chen, S.J. Feng, S. Ran, D.C. Zhu, W. Liu, H.J.M. Bouwmeester, Conversion of methane to syngas by a membrane-based oxidation reforming process, Angew. Chem. Int. Ed. 42 (2003) 5196–5198.

[8] H. Lu, J.H. Tong, Y. Cong, W.S. Yang, Partial oxidation of methane in $Ba_{0.5}Sr_{0.5}Co_{0.8}Fe_{0.2}O_{3-\delta}$ membrane reactor at high pressures, Catal. Today 104 (2005) 154–159.

[9] Y. Zeng, Y.S. Lin, S.L. Swartz, Perovskite-type ceramic membrane: synthesis, oxygen permeation and membrane reactor performance for oxidative coupling of methane, J. Membr. Sci. 150 (1998) 87–98.

[10] H.H. Wang, Y. Cong, W.S. Yang, High selectivity of oxidative dehydrogenation of ethane to ethylene in an oxygen permeable membrane reactor, Chem. Commun. (2002) 1468–1469.

[11] Y. Teraoka, T. Nobunaga, N. Yamazoe, Effect of cation substitution on the oxygen semi permeability of perovskite-type oxides, Chem. Lett. 3 (1988) 503–506.

[12] L. Qiu, T.H. Lee, L.M. Liu, Y.L. Yang, A.J. Jacobson, Oxygen permeation studies of $SrCo_{0.8}Fe_{0.2}O_{3-\delta}$, Solid State Ionics 76 (1995) 321–329.

[13] V.V. Kharton, A.A. Yaremchenko, A.V. Kovalevsky, A.P. Viskup, E.N. Naunovich, P.E. Kerko, Perovskite-type oxides for high-temperature oxygen separation membranes, J. Membr. Sci. 163 (1999) 307–317.

[14] C.S. Chen, W. Liu, S. Xie, G.G. Zhang, H. Liu, G.Y. Meng, D.K. Peng, A novel intermediate temperature oxygen permeable membrane based on the high T_c superconductor $Bi_2Sr_2CaCu_2O_8$, Adv. Mater. 12 (2000) 1132–1134.

[15] Z.P. Shao, G.X. Xiong, J.H. Tong, H. Dong, W.S. Yang, Ba effect in doped $Sr(Co_{0.8}Fe_{0.2})O_{3-\delta}$ on the phase structure and oxygen permeation properties of the dense ceramic membranes, Sep. Purif. Technol. 25 (2001) 419–429.

[16] J.H. Tong, W.S. Yang, B.C. Zhu, R. Cai, Investigation of ideal zirconium-doped perovskite-type ceramic membrane materials for oxygen separation, J. Membr. Sci. 203 (2002) 175–189.

[17] J.H. Tong, W.S. Yang, R. Cai, B.C. Zhu, G.X. Xiong, L.W. Lin, Investigation on the structure stability and oxygen permeability of titanium-doped perovskite-type oxides of $BaTi_{0.2}Co_xFe_{0.8-x}O_{3-\delta}$ ($x = 0.2$–0.6), Sep. Purif. Technol. 32 (2003) 289–299.

[18] V.V. Kharton, A.L. Shaula, F.M.M. Snijkers, J.F.C. Cooymans, J.J. luyten, A.A. Yaremchenko, A.A. Valente, E.V. Tsipis, J.R. Frade, F.M.B. Marques, J. Rocha, Processing, stability and oxygen permeability of $Sr(Fe, Al)O_{3-\delta}$ based ceramic membranes, J. Membr. Sci. 252 (2005) 215–225.

[19] U. Balachandran, J.T. Dusek, P.S. Maiya, B. Ma, R.L. Mieville, M.S. Kleefisch, C.A. Udovich, Ceramic membrane reactor for converting methane to syngas, Catal. Today 36 (1997) 265–272.

[20] H. Dong, Z.P. Shao, G.X. Xiong, J.H. Tong, S.S. Sheng, W.S. Yang, Investigation on POM reaction in a new perovskite membrane reactor, Catal. Today 67 (2001) 3–13.

[21] J.H. Tong, W.S. Yang, R. Cai, B.C. Zhu, L.W. Lin, Novel and ideal zirconium-based dense membrane reactors for partial oxidation of methane to syngas, Catal. Lett. 78 (2002) 129–137.

[22] H.H. Wang, Y. Cong, W.S. Yang, Investigation on the partial oxidation of methane to syngas in a tubular $Ba_{0.5}Sr_{0.5}Co_{0.8}Fe_{0.2}O_{3-\delta}$ membrane reactor, Catal. Today 82 (2003) 157–166.

[23] H.J.M. Bouwmeester, Dense ceramic membranes for methane conversion, Catal. Today 82 (2003) 141–150.

[24] F.T. Akin, J.Y.S. Lin, Oxygen permeation through oxygen ionic or mixed-conducting ceramic membranes with chemical reactions, J. Membr. Sci. 231 (2004) 133–146.